

# Research Journal of Pharmaceutical, Biological and Chemical Sciences

## Bismuth (0) Nanoparticle as Anti-Breast Cancer Agent Synthesis and Investigation.

Sarah Ashour Hamood\*, and Ziad Tarik Aldahan.

Al-Nahrain University, College of engineering, Biomedical Engineering Department, Baghdad, Iraq.

### ABSTRACT

We introduced a simple chemical method to synthesize semimetal bismuth nanoparticles in N,Ndimethylformamide(DMF) by reducing  $\text{Bi}^{+3}$  with sodium borohydride ( $\text{NaBH}_4$ ) in the presence of poly-(vinylpyrrolidone) (PVP) at room temperature, bismuth nanoparticle size carried out through, this method considered as well as economic method to obtain the bismuth (0) nanoparticles. The  $\text{Bi}^0$  nanoparticle compound was characterized in high performance instruments such as the X-Ray diffraction (XRD), Scanning electron microscopy (SEM), Atomic force microscopy (AFM), Fourier transfer infrared (FTIR), Ultra violet visible spectroscopy (UV/VIS spectroscopy), Thermal geometric analysis (TGA), Differential scanning calorimetry (DSC), and the anticancer activity by breast cell line. The anticancer activity showed the best performance of inhibition of cell line MCF-7 with 48 hours of treatment.

**Keywords:** Bi(0), breast cancer, bismuth nanoparticales

*\*Corresponding author*

## INTRODUCTION

The materials with a crystalline properties exhibit a variety of interesting optical, electronic, and magnetic features when the physical size of the crystalline approaches to the nanometer scale [1]. Bismuth is a semimetal with a rhombohedral structure. It has a small energy overlap between the conduction and valence bands, high carrier motilities, highly anisotropic Fermi surface, and small effective mass. As the crystalline size decreases, the induced semimetal semiconductor transition would be possible. This size induced semimetal to semiconductor transition and the related quantum confinement effects are potentially useful for optical and electro-optical device applications. Recent work also has suggested that Bi materials of reduced dimensions may exhibit enhanced thermoelectric properties at room temperature. Metal nanoparticles such as zinc oxide (ZnO), Ag, silver oxide (Ag<sub>2</sub>O), silicon (Si), titanium dioxide (TiO<sub>2</sub>), copper oxide (CuO), Au, calcium oxide (CaO) and magnesium oxide (MgO) were identified to have antimicrobial activity [2]. The metallic nanoparticles have a potential application in cancer diagnosis field, for example magnetic resonance imaging (MRI) and colloid mediators in cancer magnetic hyperthermia. The advantage of metallic nanoparticles as probes for cancer therapy is largely derived from their ability to carry a large dose of drug that result in a high concentration of anticancer drugs at the desired site, thereby avoid toxicity and other painstaking adverse effects resulting from high drug concentration in other parts of the body [3]. The most diamagnetic of all metals and the thermal conductivity is lower than any metal except mercury. Bismuth has gained significant ground as an alternative material to gold. This is owing to the low cost of bulk elemental of bismuth and its compounds. Bismuth has high x-ray opacity, as well as its generally accepted biological tolerance, making bismuth a very suitable candidate for medical X-ray contrast applications. It has a high electrical resistance, and has the highest Hall Effect of any metal (that is, the greatest increase in electrical resistance when placed in a magnetic field). It's stable to oxygen and water but dissolves in concentrated nitric acid. All bismuth salts form insoluble compounds when put into water.

In this paper, we introduce a new simple chemical method to synthesize semimetal Bi nanoparticles in *N,N*-dimethylformamide (DMF) solution by reduction of Bi<sup>3+</sup> using sodium borohydride (NaBH<sub>4</sub>) in the presence of poly(vinylpyrrolidone) (PVP). One can easily prepare the high crystalline Bi nanoparticles in narrow size distribution, high dispersibility and single phase purity. More importantly, the diameter of bismuth nanoparticles can be 50-90 nm. In particular, we also report infrared spectra (IR) of the pure PVP, as well as the UV/Vis spectroscopy show the absorbance, XRD, and the TGA to characterize the properties of nanoparticle resulted and tested on the breast cancer cell line MCF-7 to show the cancer activity on that type of cell.

## EXPERIMENTAL WORK

### Chemicals

Bi(NO<sub>3</sub>)<sub>3</sub> was used as precursors of Bi nanoparticles. Sodium borohydride (NaBH<sub>4</sub>) was used as a reducing agent. *N,N*-Dimethylformamide (DMF, 99.9%, water < 0.005%) and poly(vinylpyrrolidone) (PVP, *M<sub>w</sub>* 55 000) were used as solvent and stabilizer, respectively. All of these high grade chemicals were purchased from Aldrich Chemical Company. The synthesis of Bi NPs confirm by the reaction of (4.859, 0.1 mmol) from bismuth nitrate hydrate ((BiNO<sub>3</sub>)<sub>3</sub>·5H<sub>2</sub>O) dissolved in 20 ml dimethylformamide (DMF), the Polyvinylpyrrolidone (PVP) was dissolved in (10 ml) of (DMF) which was stirred and protected from atmospheric air by nitrogen blanket. The amount of (PVP) was elevated from (0.555 to 55.5 mg) about (0.5 mmol) as monomeric unit. Then the (0.3 ml) of (1.0 M) of aqueous solution of the reduction agent (NaBH<sub>4</sub>) was injected into (10 ml) of (DMF) and also degassed by using the nitrogen atmosphere for 15 minutes, the solution containing (DMF) and (NaBH<sub>4</sub>) was added to the mixture of (Bi(NO<sub>3</sub>)<sub>3</sub>·5H<sub>2</sub>O) and (PVP) in the (DMF) solution under stirring and nitrogen blanket, After a few minutes observed the solution become black in color. The stirring continued with 5 minutes after the color is change, the bismuth nanoparticles was precipitated from solution inducing the Bi NPs were obtained the acetone was added to complete the precipitation, drying the particles and confirmed with available measurements to evidences the size and the formation of Bi NPs.

### MTT assay

Colorimetric for assessing cell metabolic activity. NAD(P)H-dependent cellular oxidoreductase enzymes may, under defined conditions, reflect the number of viable cells present. These enzymes are capable

of reducing the tetrazolium dye MTT3-(4,5-dimethylthiazol-2-yl)-2,5 diphenyltetrazolium bromide to its insoluble formazan, which has a purple color. MCF-7 cells and MCF-10A cells were seeded separately in 96-well plate ( $0.8 \times 10^4$  cells/well) in triplicate and incubated for 24 h to be attached to the plates. After incubation for 24 hours, cells were treated with increasing concentrations (2.5, 5, 10, 20 nM) [4-6] of bismuth nanoparticles for 12, 24, 48 and 72 hours, respectively for the detection of prepared sample. After respective incubation periods, 20  $\mu$ L of MTT (1 mg/mL) was added to each well and incubated for 4 h at 37°C. Then the formazan crystals formed by the viable cells were dissolved by the addition of 200  $\mu$ L of DMSO to each well and the color intensity value of the processed cells was measured at 550 nm that present the cell survival percentage in corresponding wells in contrast with their respective controls. The same procedure was done for MTT assay for human normal breast cell line [7,8].

### RESULTS AND DISCUSSION

The UV-Vis spectrum of Bi NP compound figure (1) in DMSO solvent displayed the characteristic peak at (317 nm) with absorbance (1.05) according to the Beer Lambert's law [9,10]. The extension molar coefficient is equal to (1050) ( $\text{mol}^{-1} \cdot \text{L}^{-1} \cdot \text{cm}^{-1}$ ). This value with a good agreement of bismuth nanoparticle molecule were the curve performed that illustrate from the ratio of absorbance between the PVP and the Bi NP to the wavelength [11,12].

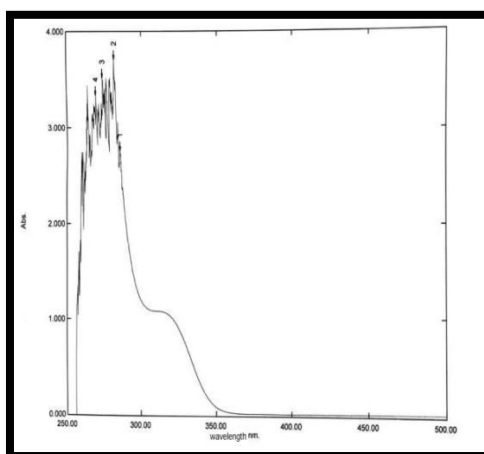


Figure 1

while FT-IR spectrum of Bi NPs shown in figure (2) shows the characteristic bands at (1647)  $\text{cm}^{-1}$ , (1383)  $\text{cm}^{-1}$ , (1003)  $\text{cm}^{-1}$  and (543)  $\text{cm}^{-1}$  due to the purity of nanoparticle of bismuth compound attached to the physical binding with polyvinylpyrrolidone (PVP), this property illustrate the ability of Bi NP liberated from solution as ( $\text{Bi}^0$ ) and attached with target as single compound [13,14].

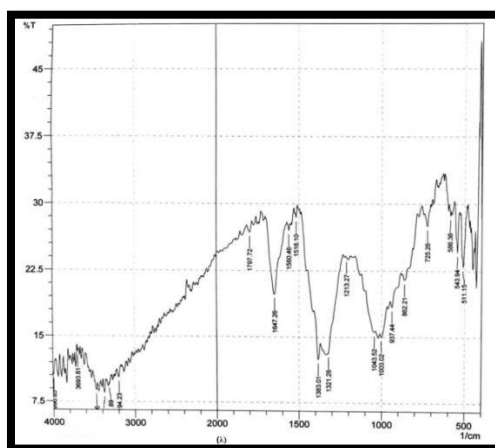


Figure (2) FTIR spectrum of Bi NPs

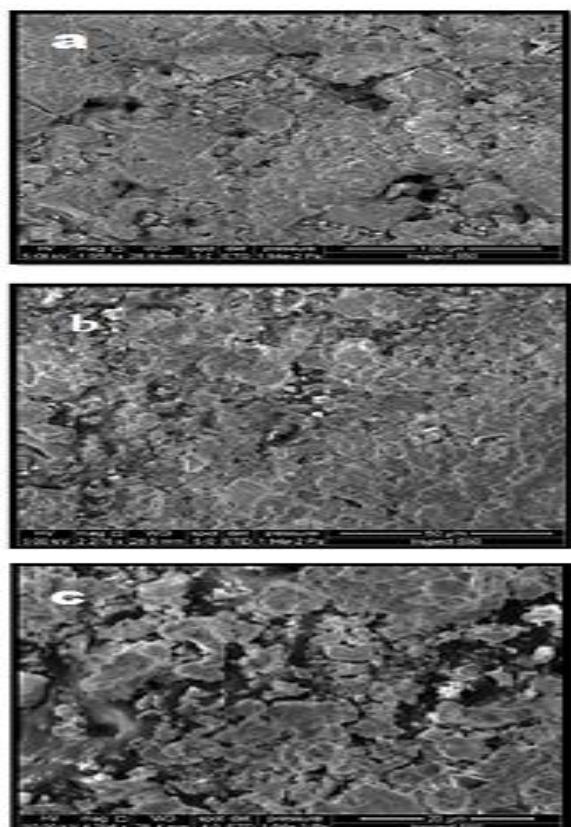


Figure (3) SEM of Bi NPs at magnifications power (a) 1055x, (b) 2276x and (c) 4756x

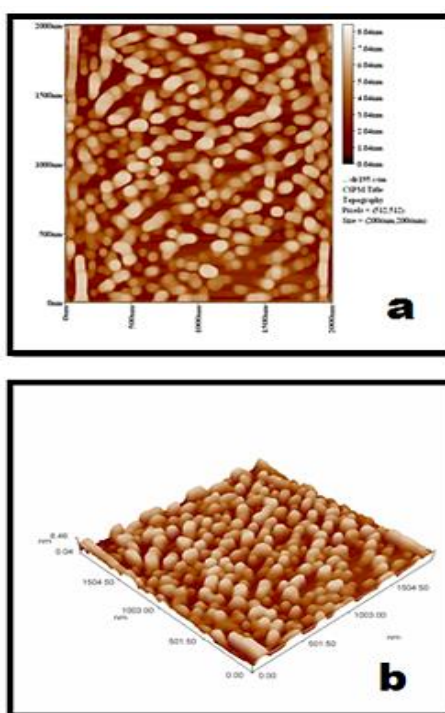


Figure (4) AFM of Bi NPs (a) deposited on slide, (b) 3-D image of Bi NPs

The scanning electron microscopy (SEM) was used to determine the shaped size and morphology of bismuth to give image with high resolution of the sample surface and packed of molecules by magnifying up to 200k times [15,16], the SEM test figure ((3) a, b and c) illustrate the packed type of bismuth nanoparticle

molecule in different wavelengths at ( 100 μm, 50 μm and 20μm respectively ), since it's very clearly shows the crystallinity and property of molecule in different size as nanoparticle.

The atomic force microscopy AFM as used to provide the more evidence and more details of the size and molecular distribution of particles by resolving individual particle and groups in the three dimension analysis [17,18] figure ((4) a and c) shows the two and 3D dimensions of sample also the granulite Cumulating destitution explain clearly distribution of particles according to the diameter which that shows the size of particles a highly percentage with (75nm) and (80 nm) with average size are (77.82 nm) diameter[19].

The XRD technique used to characterize the crystallinity and amorphous properties, figure (5) displayed the XRD of bismuth nanoparticle, which shows the crystalline property due to the beaks (27) and (28) as twin beaks in different intensity and the beaks at (38), (40) and (48) due to the arrange crystalline property with the 2θ degrees of the sample, this measurement give a significant values corresponding with the SEM and AFM measurements [20-22].

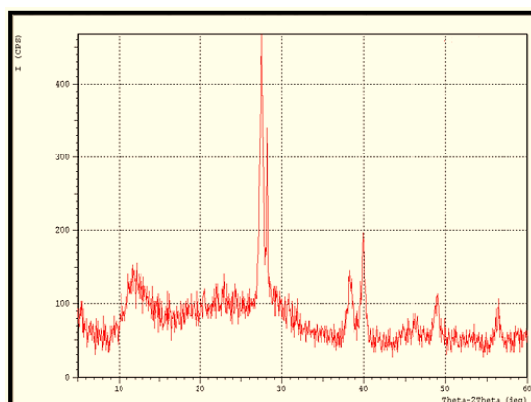


Figure (5) X-Ray diffraction for Bi NPs

The particle of the sample bismuth nanoparticle was tested by TGA evaluated the thermal behavior graduated heating process between (0 – 400 °C), since the figure (7) shows the weight losing of the sample with elevated temperature degree, the good absorption, the sample is more stable shows is the weight losing started with (335.5 °C) as (0.42 mg) comparison with staring weight (22 mg). This value reflected the stability of the prepared compound in highly temperature degree; As a result, thermal scan was recorded as plot of heat flow versus temperature [23].

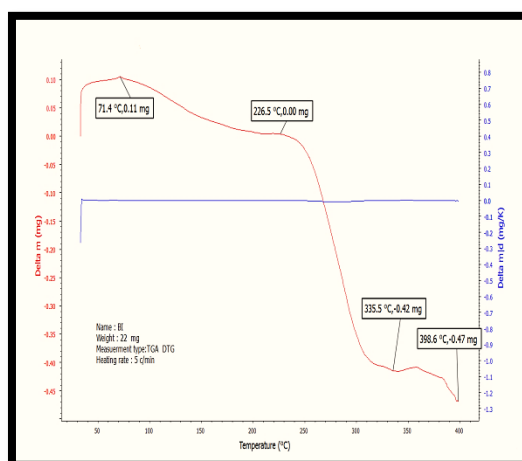
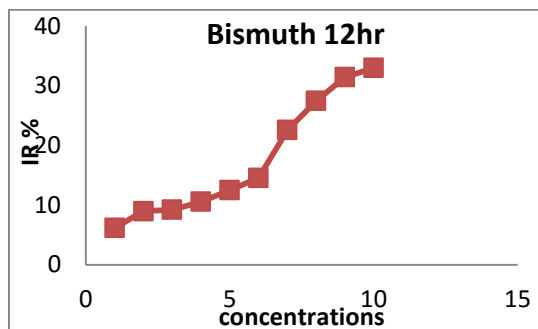


Figure (7) Thermal Gravimetric Analysis graph of Bi NPS

In the current study, it was found that there were an obvious concentration related cytotoxic effects of bismuth nanosized particles at 12hrs exposure times. At 12 hrs exposure time, one can easily inspect the

inhibition rate percent (IR%) of breast cancer line at different concentrations which was increased with increasing the concentrations as seen in the figure (8).



Figure(8) The I.R % versus Concentrations at 12 hrs Exposure time

The inhibition rates percent (I.Rs%) were (6.16688, 8.99213, 9.2299, 10.5556, 12.4897, 14.5678, 22.5677, 27.4555, 31.4333, 32.98889 %) as compared to control two . The concentration dependent anti-proliferative effects of the test compound suggested an increase in the uptake of such material Bi NPs with increasing the concentration This results in leaky, defective vessels and impaired lymphatic drainage. Nanoparticles sized at 10 to 100 nm have the ability to accumulate within tumors because of their ineffective lymphatic drainage. Thus, consideration of the size and surface properties of nanoparticles is vital, particularly for passive targeting. Particles must be less than 100 nm to avoid uptake by the reticulo-endothelial system and their surface should be hydrophilic to avoid rapid clearance by macrophages [24]. While the effect of bismuth nanoparticles on the MCF-7 showed the results the fluctuated I.Rs% at 24 hrs exposure time, the bismuth still experienced anti-proliferative activity, but such growth inhibitory effects were not regular owing to some defense mechanisms or adapted mechanisms that were able to make the cells to efflux the foreign materials outside the cells, the nanosized metals may subjected to exocytosis and moving out of the cells and about 66% of endocytosed nanoparticles where exocytosed by 48 hours compared to an exocytosis of ~ 10% at 2 hours. A long incubation period of 48 hours was taken to expel 66% of the particles endocytosed in 2 hours, implying a slow exocytosis rate than endocytosis [25]. A significant amount of endocytosed nanoparticles (34%) was still retained by the cells and these findings explain the fluctuations in the results showed in the figure(9).

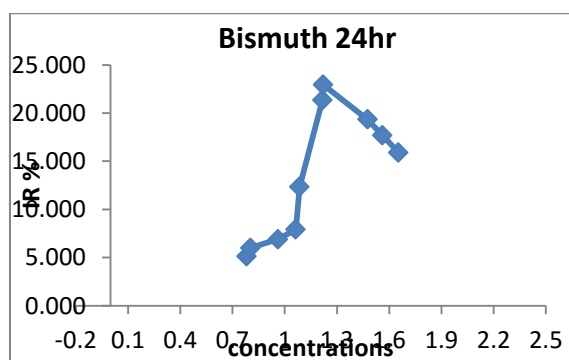


Figure (9) The I.R % versus Concentrations at 24 hrs Exposure time

At 48 hrs exposure time the I.Rs % were shown to be markedly decline after 41.69 concentration where the inhibition rate percent was 40% till reaching 10% at 11.50 concentration, such decline in the growth inhibition [26], the fact that (Bi) is (a trivalent heavy metal) that is used to treat gastrointestinal infection. Bismuth drugs display high selectivity for pathogenic cells but have low toxicity to human cells. While bismuth cellular uptake and disposal mechanisms are unknown, the Bi<sup>+3</sup> ion has high affinity toward glutathione. The relationship between the two and quantitatively determined the metabolism of bismuth in human cells [27]. The researchers found that in humans, bismuth uptake first follows a saturation pattern of passive transport. During this time, bismuth uses approximately half of the intracellular glutathione that is present. This phase is followed by exponential growth, during which glutathione levels increase over 4-fold from the original levels.

The authors looked at how glutathione depletion affected bismuth metabolism and found that it dramatically reduced bismuth uptake and that bismuth-treated, glutathione depleted cells exhibited disturbed morphology with lower survival rates. Furthermore, they discovered that glutathione is essential to bismuth subcellular compartmentalization, which protects cells from acute toxicity. The researchers found that after bismuth is passively absorbed by human cells, the vast majority of it is conjugated to cytosolic glutathione and then transported into perinuclear vesicles; in a self-sustaining positive feedback process, this glutathione sequestration activates de novo biosynthesis, which facilitates passive uptake of bismuth. Glutathione is absent from many Gram-positive bacteria which may explain bismuth drug selectivity, therefore now, we can easily explained the decline in the growth inhibition rate percentage (I.Rs%) being a saturable mechanism (i.e. uptake of bismuth can be saturated in case of over exposure to bismuth [28]. Consequently the fall in the above curve would proceed till the saturation terminated figure (10).

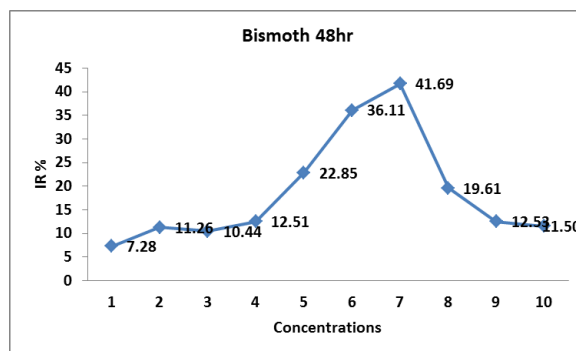


Figure (10) The I.R % versus Concentrations at 48 hrs Exposure Time.

### CONCLUSION

The synthesis of bismuth nanoparticles was performed by physical complex without any reaction on their function group which was approved by FT-IR, SEM, AFM, XRD and TGA, bismuth nanoparticle showed non-significant change in solubility, but increase in its antitumor activity MCF-7 cell line accompanied with high significant (8) and the most effect time accrued at 48 hrs with maximum inhibition rate (IR%) 41.69% reduction in its undesirable cytotoxic effect on the normal mammary cell line (MCF-10A) with non-noticed side effect of drug of metal nanoparticle.

### REFERENCES

- [1] Rai M, Yadav A, Gade A., *Biotechnology advances*. 2009;27(1):76-83.
- [2] Besinis A, De Peralta T, Handy RD., *Nanotoxicology*. 2014;8(1):1-6
- [3] Ahmad MZ, Akhter S, Jain GK, Rahman M, Pathan SA, Ahmad FJ, Khar RK., *Expert opinion on drug delivery*. 2010;7(8):927-942.
- [4] Adesina SK, Holly A, Kramer-Marek G, Capala J, Akala EO., *Journal of pharmaceutical sciences*. 2014;103(8):2546-2555.
- [5] Liebmann JE, Cook JA, Lipschultz C, Teague D, Fisher J, Mitchell JB., *British journal of cancer*. 1993;68(6):1104-1108.
- [6] Esfandyari-Manesh M, Mostafavi SH, Majidi RF, Koopaei MN, Ravari NS, Amini M, Darvishi B, Ostad SN, Atyabi F, Dinarvand R., *DARU Journal of Pharmaceutical Sciences*. 2015;23(1):1-3.
- [7] Wang L, Li H, Wang S, Liu R, Wu Z, Wang C, Wang Y, Chen M., *AAPS PharmSciTech*. 2014;15(4):834-844.
- [8] Lin Y, Jiang D, Li Y, Han X, Yu D, Park JH, Jin YH., *Journal of ginseng research*. 2015;39(1):22-28.
- [9] Kaur P, Chandel M, Kumar S, Kumar N, Singh B, Kaur S., *Food and chemical toxicology*. 2010;48(1):320-325.
- [10] Dawood HA, Khalaf R, Salman Z. *Iraqi National Journal of Chemistry*. 2009;35(1):489-491.
- [11] Khan M, Khan M, Kuniyil M, Adil SF, Al-Warthan A, Alkhathlan HZ, Tremel W, Tahir MN, Siddiqui MR. *Dalton Transactions*. 2014;43(24):9026-9031.
- [12] Bonferoni M., Sandri G., Dellera E., Rossi S., Ferrari F., Mori M., Caramella C. *European Journal of Pharmaceutics and Biopharmaceutics*. 2014; 87(2014):101-106.

- [13] Shao L, Susha AS, Cheung LS, Sau TK, Rogach AL, Wang J., Langmuir. 2012;28(24):8979-8984.
- [14] Dawood AH, Kareem ET, Madlool AM. International Journal of Chemistry. 2012;4(6):64-66.
- [15] Heera, P. and Shanmugam S., Int. J. Curr. Microbiol. App. Sci, 2015; 4(8): 379-386.
- [16] Pal SL, Jana U, Manna PK, Mohanta GP, Manavalan R. Journal of Applied Pharmaceutical Science. 2011;1(6):228-34.
- [17] Butt HJ, Jaschke M. Calculation of thermal noise in atomic force microscopy. Nanotechnology. 1995;6(1):1-5.
- [18] Moosa, A.A., A.M. Ridha, and M. Al-Kaser,. International Journal of Multidisciplinary and Current research, 2015. 3(2015):966-975.
- [19] Tamayo J, Humphris AD, Owen RJ, Miles MJ. Biophysical journal. 2001 Jul 31;81(1):526-537.
- [20] Bhowmick S. International Journal of Engineering. 2012;5(1):1-2.
- [21] Snellings R, Machiels L, Mertens G, Elsen J., Geologica belgica. 2010;13(3):183-196.
- [22] Bish DL, Post JE. Modern powder diffraction. Washington, DC: Mineralogical Society of America; 1989;pp.275-279.
- [23] Sierra-Ávila R, Pérez-Alvarez M, Cadenas-Pliego G, Padilla VC, Ávila-Orta C, Camacho OP, Jiménez-Regalado E, Hernández-Hernández E, Jiménez-Barrera RM. Journal of Nanomaterials. 2015;2015(1):140-144.
- [24] Roco MC. Current opinion in biotechnology. 2003;14(3):337-346.
- [25] Asharani PV, Hande MP, Valiyaveetil S., BMC cell biology. 2009;10(1):1-3.
- [26] Shudofsky AM, Silverman JE, Chattopadhyay D, Ricciardi RP. Journal of virology. 2010;84(23):12325-12335.
- [27] Hong Y, Lai YT, Chan GC, Sun H., Proceedings of the National Academy of Sciences. 2015;112(11):3211-3216.
- [28] Zhi H, Zahoor MA, Shudofsky AM, Giam CZ., Oncogene. 2015;34(4):496-505.